

How to perform adequate optical  
strain measurements  
on a  
sheet metal truck bumper

Sil Bijker  
Report MT06.56

How to perform adequate optical strain measurements  
on a  
sheet metal truck bumper

Sil Bijker  
Report MT06.56

Coach: Dr. Ir. R.H.J. Peerlings  
Eindhoven, December, 2006

Eindhoven University of Technology  
Department of Mechanical Engineering  
Division of Computational and Experimental Mechanics

# Contents

1	Introduction.....	3
2	The ARGUS system.....	4
3	Taking pictures.....	7
3.1	USING A STANDARD DIGITAL CAMERA .....	8
3.2	POSITIONING OF THE MARKERS .....	8
3.3	ILLUMINATION .....	9
3.4	CAMERA POSITIONS.....	10
3.5	MEASURING LARGE OBJECTS.....	10
4	Processing the photographic data.....	11
4.1	CAMERA PARAMETERS .....	11
4.2	STEP ONE: ‘COMPUTE ELLIPSES AND BUNDLE’ .....	12
4.3	STEP TWO: ‘COMPUTE 3D-POINTS AND GRID’ .....	13
5	Strain measurement results for the bumper .....	14
5.1	RESULTS REGION 1 .....	16
5.2	RESULTS REGION 2.....	18
5.3	RESULTS REGION 3.....	19
5.4	LAMPHOLE .....	20
5.5	COMPLETE ETCHED REGION .....	23
5.6	VALIDATION OF THE LS-DYNA RESULTS.....	24
6	Conclusion and recommendations .....	27
7	Bibliography .....	29

# Chapter 1

## Introduction

The production of a sheet metal bumper consists out of several production steps that finally lead to the bumper geometry. In this report a Daf XF bumper with a thickness of 2 mm is considered. In the production steps of the bumper, thickness reduction, residual stresses and hardening of the material may occur. To investigate this, numerical models have been created that simulate the production steps of the bumper. The models were built in LS-Dyna, see [2]. To validate the models, use has been made of an optical strain measurement technique that is implemented in the so called ARGUS system.

This report is about making such an optical strain measurement in an adequate way. ARGUS measures the strains by computing the distances between the dots of a grid. Before the production steps of the bumper, this grid is etched onto the undeformed sheet metal and it deforms together with the sheet metal during the production steps. By taking several pictures of the bumper and its deformed grid of dots, the ARGUS system can for example compute the major and minor strain and thickness reduction of the bumper.

Several influences, such as bad illumination, low quality dots or misplaced markers, may lead to a poor measurement. In this report these influences will be discussed and the final results will be shown, including a comparison with the LS-Dyna results. The measurements have been carried out in the multiscale lab at the Technical University of Eindhoven (TU/e).

# Chapter 2

## The ARGUS system

Gom<sup>1</sup> is a manufacturer of optical measurement systems. One of its products is ARGUS, an optical measuring technique to determine form changes in sheet metal components. ARGUS can compute for example major strain, minor strain, thickness reduction and the component's geometry. It is also possible to construct a Forming Limit Diagram (FLD) if the material properties are known.

The working principle of the ARGUS system is based on photogrammetry, also called remote sensing. This method allows one to compute a three-dimensional geometry on the basis of a set of two-dimensional pictures. Because the ARGUS system works in grey scales, the pictures must be in black and white. The location of spatial points of an object is determined by using a triangulation of directional light bundles. This can be explained

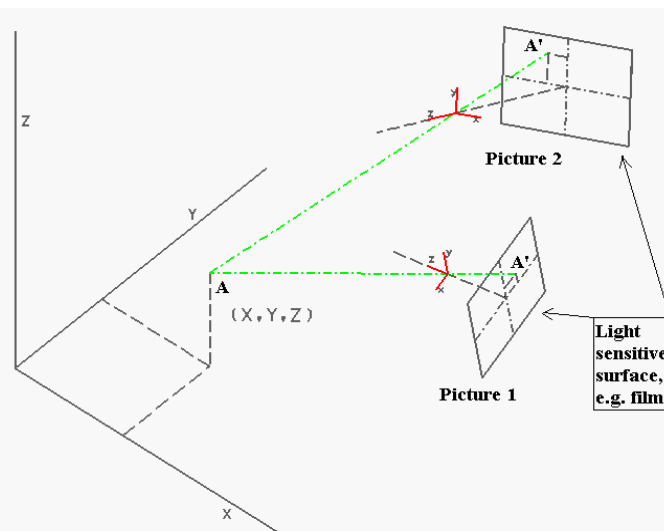


Fig. 1 Coordinate determination of point A using photogrammetry.

<sup>1</sup> Gom GmbH in Braunschweig, Germany. Website: [www.gom.com](http://www.gom.com)

by Fig. 1, where a schematic representation of the photogrammetry principle is given. In this figure the spatial point A in the three-dimensional space  $(x,y,z)$  is determined by two pictures. Each picture is taken from a certain position and viewing direction in space. This position and view direction is given by the camera coordinate system, which is indicated by the red axes in Fig. 1. The origin of the camera coordinate system corresponds to the camera's lens, with the z-axis normal to the lens and light sensitive surface. The distance between the origin of the camera coordinate system and the middle of the light sensitive surface must be regarded as the focal length of the camera. With this information it is possible to construct a line that goes through point A' on the light sensitive surface and the origin of the camera coordinate system. This is the green line that is drawn for both pictures in Fig. 1. The coordinates of point A can now be determined by the intersection of the two green lines.

In the previous example three parameters were necessary to determine the three-dimensional coordinates of point A, namely the camera position and view direction (*n exterior orientations*), the coordinates of point A' on the light sensitive surface (*Image coordinates of n views*) and the focal length of the camera (*inner orientation*). This is also shown in Fig. 2 where *inner orientation* is replaced by *camera models*. Each of the four main variables can be an input or a result of a photogrammetric method. Furthermore *additional observations* play an important role: using scale bars, i.e. a known distance of two points in space, or known fixed points, a connection to the basic measuring units is created. In the ARGUS system first a method is used to determine the *n exterior orientations*, for which the system uses the unique markers and scale bars that must be fixated on the object to be measured. With the *n exterior orientations* available, it is possible to determine the *three dimensional coordinates* of several points on the object.

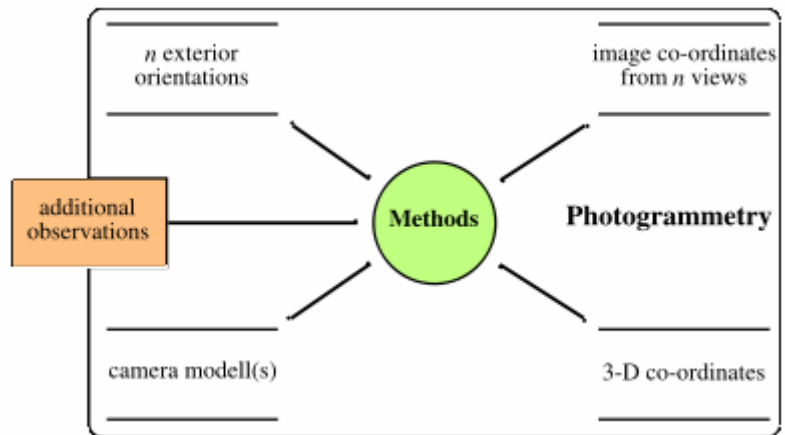


Fig. 2 Wiora's data model of photogrammetry. Source [6]

To measure strains at the surface of the object it is necessary that a grid of dots is clearly visible on the object. The regular grid of dots is etched onto the unprocessed steel blank. While forming the object, the grid deforms together with the blank, and it thus contains the necessary strain information. Note that as a result of the deformation dots can become ellipses. In Fig. 3 on the next page a dot pattern is shown. The used dot pattern has a diameter of 1.5 mm and has a centre to centre distance of 3 mm. Etching the grid of dots is an electrochemical process which is also called electrolytic marking. Two types of

etching can be distinguished; black etching in case of steel or white etching if the material is aluminum.

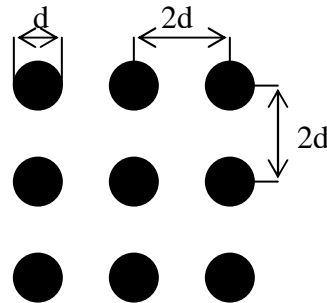


Fig. 3 Used dot pattern

Every ARGUS system comes with circular barcode markers. These markers must be placed in the region of interest and are required for calculating the camera position with respect to the object for each picture. At the TU/e there are two sets of markers present; one set for steel and one for aluminum objects. Both sets are 10-bit, which means that one set contains 100 unique markers. For large objects there is a 12 bit or a 15 bit set of markers available with respectively 300 and 429 unique markers. In Fig. 4 a typical marker is shown. The camera position is found by precisely determining the centre of each marker, while the broken circle around the centre enables the software to attribute an unambiguous ID to the marker. The set of barcode markers also contains two scale-

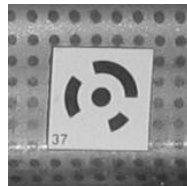


Fig. 4 Typical marker, magnetically placed on the object surface.

bars. A scale-bar consists of two unique markers that have a known and fixed distance. At least one scale-bar must be placed on the object of measurement. The coordinates of the two unique markers of the scale-bar must be determined in order to be able to scale the measurement to real-world coordinates. If this is omitted, a correct calculation of the strains is impossible. This is because the strain is determined by comparing the distance between the dots in the deformed case with the original distances which must be entered before the strain computation.

# Chapter 3

## Taking pictures

Taking the digital photographs can be regarded as the most important step in obtaining good measurement results. Pictures of a low quality have a considerable negative influence on the computation of the grid. If for instance certain areas of the image are under- or overexposed, the dots have insufficient contrast and so the computation may fail in that area, leaving gaps in the computed grid.

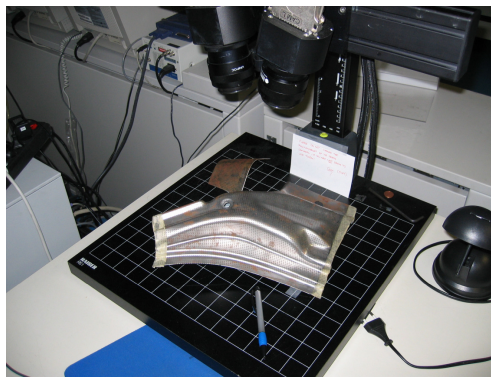


*Fig. 5 Vosskuhler CCD 1300 camera belonging to the ARGUS system*

The ARGUS system is equipped with a Vosskuhler CCD 4000 camera. This camera is fixed onto a stand as shown in Fig. 5. This setup is adequate for small or medium size objects but not for a truck bumper because it is not practical to photograph the bumper from every direction using a fixed camera position. To overcome this difficulty, use has been made of a 'normal' hand held digital camera. The following section will give more information about using an ordinary digital camera for a measurement with ARGUS.

The purpose of this chapter is to explain how to obtain a proper set of pictures. Therefore camera positions, illumination and positioning of the markers are discussed. The final subject of this chapter is how to deal with relatively large measurement objects.



### 3.1 Using a standard digital camera

For photogrammetry purposes the used digital camera is not optimal because the internal geometry of such a camera is not known accurately enough. Metric cameras must be used if this high accuracy is desirable. Metric cameras have precisely known internal geometries and very low lens distortions. To obtain the highest accuracy using the standard camera no zoom function has been used, keeping the widest possible angle with a focal length of 7.4 mm. For the photogrammetry calculations the ARGUS software needs to be provided with the camera's focal length, pixel resolution and its pixel size. If these quantities are not correctly entered, this may lead to poor results or even to no results at all. One should keep in mind in this connection that when the zoom function of the camera is used the focal length changes. Therefore it is advisable to keep the zoom function in the widest possible angle during the measurement.

The dots or ellipses in a picture must contain a certain number of pixels to be identified by the ARGUS software. If the ellipses have a diameter of ten or more pixels, the ellipse finder may not work because of the graylevel distribution inside the ellipses. They may also not be smaller than five pixels because otherwise the graylevels of the object and its surroundings introduce false ellipses. The mentioned pixel values can change if the default settings are adjusted.

### 3.2 Positioning of the markers

As mentioned in chapter 2, markers are necessary for the ARGUS software to calculate the camera position in each image. The markers have been printed on magnetic foil so they adhere to objects made of steel. They are to be distributed around the area to be measured in such a way that at least five markers are visible from each perspective and that these markers are not in a straight line. It is safer to have more than five markers visible. For a better computation of the camera positions it is wise to place some additional markers at a little distance from the measurement area, preferable in a way that they are not lying in one plane with the other markers. Fig. 6 shows an example of marker positioning.



*Fig. 6 Example of how the markers could be placed. Note that the markers do not have to be directly on the object's surface.*

As the picture shows, it is not necessary to place the markers directly on the object's surface. During the measurement, the markers may not be moved with respect to each other and with respect to the etched pattern on the sheet metal. This is no issue if all markers are fixed directly onto the object surface. However if this is not the case, like in Fig. 6, care must be taken not to move the object or the markers. If movement has taken place, the system may be divergent and no camera positions can be determined.

### 3.3 Illumination

The illumination of the object is an important issue which has a crucial influence on the success of the measurement. The most desirable situation is that the area to be measured has a homogeneous distribution of light. The light being used to illuminate the object must be diffuse to limit the reflection of the steel surface. If reflections occur, no dots are visible in this area, resulting in a loss of information. Even with diffuse light reflections are inevitable, especially in corners or curved surfaces. Unfortunately these areas are often the most interesting.



*Fig. 7a Illumination setup. Creating diffuse light by using paper.*

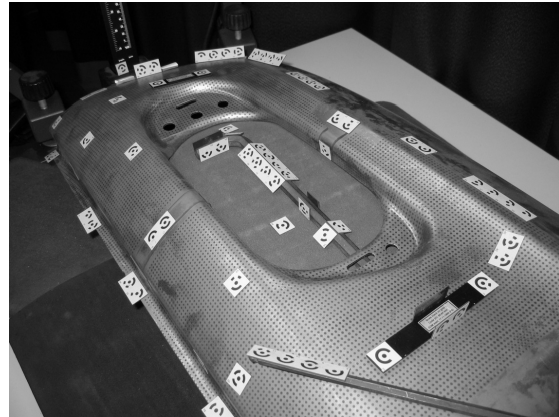


*Fig. 7b Additional markers place on a non shiny dark surface to reduce the amount of backlight.*

In Fig. 7a an example is given of how the illumination of the bumper experiments has been set up and how diffuse light has been created using paper covers of the lamps. To have full control over the illumination, measurements have been done in a dark room, so that no external light can interfere. It is preferable not to use the flash of the camera, but because of a lack of diffuse light the flash has been used with the present measurements. Fig. 7b shows that some additional markers have been placed on a dark surface to reduce the backlight. If a white background were used for the same measurement, the resulting backlight would necessitate a small camera aperture, resulting in underexposed measurement areas and poor measurements.

### 3.4 Camera positions

The camera positions must be chosen so that every image contains at least five bar-coded markers and that every etched dot is visible in at least three images taken from different directions. However, in practice it is wise to take more images in order to improve the precision and reliability of the calculated object-points. An effective method is to first create a basic set of pictures and then refine the image set as needed. The basic set can be constructed as shown in Fig. 8.

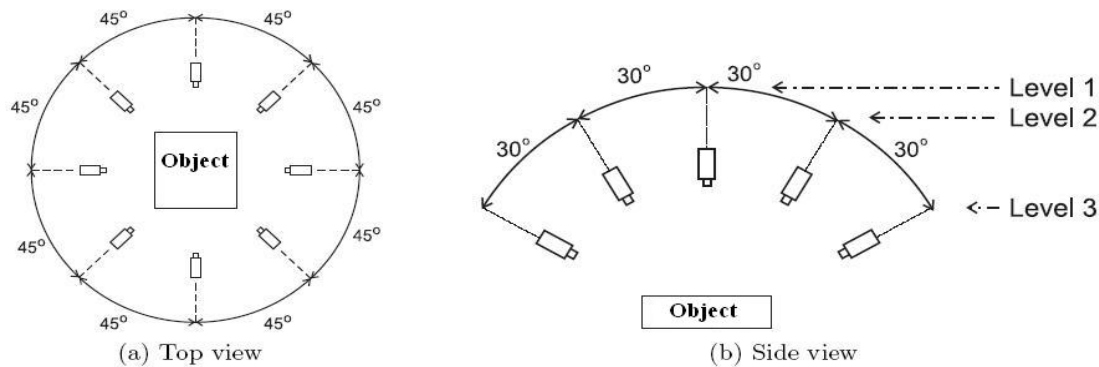


Fig. 8 Camera positions for taking pictures of the object: a top view, b side view. Source [7]

From each level as indicated in Fig. 8b pictures are taken around the object at approximately 45 degrees between each picture. The pictures should be taken from such a distance that the entire object is visible and most of the image is taken up by the object. Areas with simple geometries, e.g. flat surfaces, need fewer pictures than more complex curved geometries. If in the processing stage it turns out that there is a lack of photographic data, then additional pictures can always be taken and added to the processing. Note that while taking the additional pictures all markers must be in precisely the same positions as in the basic set of pictures.

### 3.5 Measuring large objects

Large objects can be measured with ARGUS if some additional precautions are taken. Because the marker per area ratio is smaller for large objects, more attention must be paid to placing the markers in an efficient way. This can be done by equally distributing the markers around and within the measurement area. An example is given in Fig. 7b, where the complete lamphole of the finished part has been measured at once. Markers must only be placed in the measurement area if the strains in that area are homogeneous. Only then the gap that is introduced by the marker can be interpolated safely in the post-processing stage. By using a 12 or 15 bit set of code markers it is possible to extend the measurement area further. In case of the bumper measurements the 10-bit coded-marker set was still sufficient. The basic set of pictures can be taken in the same way as described in section 3.4. Because of the size of the object it may be necessary to take the pictures from a greater distance. However, the camera resolution should then be sufficient to be able to distinguish the markers and dots, see section 3.1. Additional pictures can be taken if for a particular area the photographic data is not satisfactory. These additional pictures may be a close-ups of that particular area as long as they meet the conditions described in section 3.4. A result of a large measurement area is shown in section 5.5.

# Chapter 4

## Processing the photographic data

In the processing stage two steps can be distinguished. First the computation of the ellipses and bundles is done and then the computation of the 3D-points and grid. The former step is the most important, because it converts the photographic data to geometrical data, which is crucial for the outcome of the further computations. In this step the software tries to recognize the ellipses and bar coded markers and from them computes the three-dimensional camera positions. In the latter step the recognized ellipses are converted to 3D-points which subsequently are used to generate the grid. The grid consists of elements that are created by using the 3D-points as nodes for each element. For both these steps some useful tips will be given to improve the computational results. This chapter can be regarded as an addition to the *abridged user manual (v 5.4)* [4].

### 4.1 Camera parameters

The ARGUS program uses many parameters and settings. It is recommended to use the default setting for most of these parameters, but there are a few parameters to be known. Because use has been made of an external camera, there are three important parameters that have an influence on the computational results, namely camera resolution, focal length and the size of one single pixel of the light sensitive sensor of the camera. The most important parameter is the resolution of the camera. This must exactly correspond with the true camera setting to be able to add pictures to the ARGUS program. Also be sure that the focal length is set correctly. If the focal length does not exactly correspond with the true camera setting, this will lead to poor 3D-points and grid. In extreme cases the ‘computation of ellipses and bundle’ step may fail with the following error: [MTRITOP-CMP002 system is divergent]. This is why it is strongly recommended not to use the zoom function of the camera during the measurement. For the pixel-size parameter the same consequences hold as for the focal length. The camera settings used

for the bumper measurements are: resolution = 2272 x 1704 pixels, focal length = 7.4 mm (completely zoomed out), pixel size = 3.12  $\mu\text{m}$ .

## 4.2 Step one: ‘Compute Ellipses and Bundle’

Before step one can be taken the pictures must be uploaded to the ARGUS program. Directly after the pictures are uploaded the ARGUS program automatically starts with the determination of ellipses and markers in all of the pictures. After that choose ‘Compute Ellipses and Bundle’ from the project menu. After step one it may be necessary to ‘clean up’ some of the processed data and redo step one. This ‘cleaning up’ must be done in the ‘Project Mode’ and consists of two actions: ignoring images of poor quality and deleting or renumbering unidentified markers. Ignoring images of poor quality can be done easily by looking in the root of the image-group. The ARGUS program automatically indicates poor images with the sign as depicted in Fig. 9. These indicated images can be ignored by clicking the right mouse button on the image that needs to be ignored and choose ‘Ignore

Image 21	330	✓
Image 22	448	○
Image 23	745	○
Image 24	0	○
Image 25	693	○
Image 26	1516	○

Fig. 9 Image root. Image 24 must be ignored.

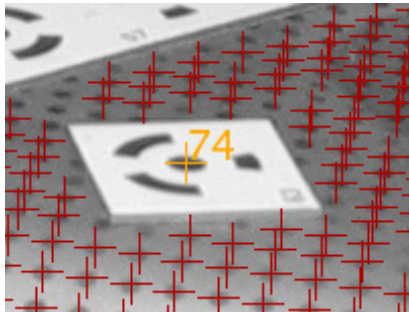


Fig. 10a Incorrect numbering of marker.



Fig. 10b Marker does not exist and must be deleted.

image’. For deleting the unidentified markers each image must be looked at separately. Be sure that ‘show unidentified points’ is turned on. Fig. 10 shows two examples of unidentified markers. Fig. 10a shows an identified marker that has an incorrect number. In this case the unidentified marker must be selected with control - left mouse button and from the “Image Point” menu “Set ID for Image Point” must be chosen. Now the correct marker number can be entered. Obviously this can only be done if the correct marker number is known, for example by inspecting the pictures or the measurement setup. Fig. 10b shows an identified marker which in reality is not a marker. These types must be deleted. These actions also are done in project mode.

After all the data has been cleaned up, step one must be repeated with “Reset all ellipses in image” turned off; otherwise all cleaning work has no effect.

### 4.3 Step two: ‘Compute 3D-Points and Grid’

In step two one image-point, which represents an ellipse, must be selected in a picture that is preferably taken from above the object. From this particular image-point the computation will start and propagation of the grid will thus start from that point. In practice step two usually has to be done several times to get a complete grid. The cause of this is that the propagation of the grid often can not proceed because there are not enough image-points available to successfully determine the 3D-point coordinates. If this is the case the 3D-point is not accepted and therefore the grid cannot be expanded further, creating a boundary of the grid. To expand the grid further, step two can be repeated at another image-point which does not belong to a grid. At the end, when no further expansion of the grid is possible, the individual grids can be combined to one single grid.

If there are still areas with no 3D-points and grid, it is possible to manually add 3D-points by selecting one individual image-point in two different pictures. This can be done by selecting an image-point and pressing control - left mouse button. In the right bottom corner of the screen a second image appears. Select another image near to the first image in the Explorer and press control - left mouse button in the right image on the same image-point as in the left image. To help find the corresponding image-point in the right image ARGUS shows a so called epipolar line. The searched image-point must lie somewhere on that line.

The last tip is to be careful with accepting a grid. Fig. 11 shows that the elements of a grid sometimes do not have the correct shape, resulting in very high and unrealistic computed strains at that particular element.

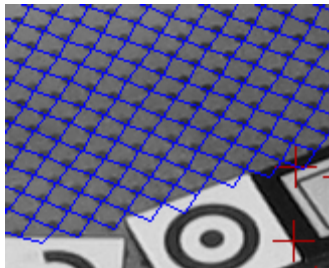


*Fig. 11a Correct grid.*

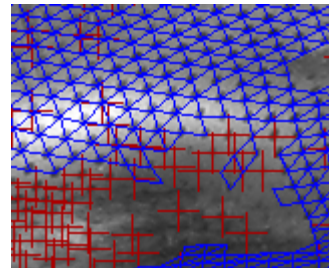


*Fig. 11b Incorrect grid.*

## Chapter 5

# Strain measurement results for the bumper

The procedure as discussed in the previous chapters has been applied to a Daf truck bumper. To obtain information on the evolution of strain during the different production steps not only the finished bumper has been measured but also a semi-finished bumper, which was obtained after the first step of the production process. In this first production step the main shape of the bumper is made by pressing the blank into a die. Also a slitting operation is used at the position of the lamphole. The second step consists of some trimming operations.

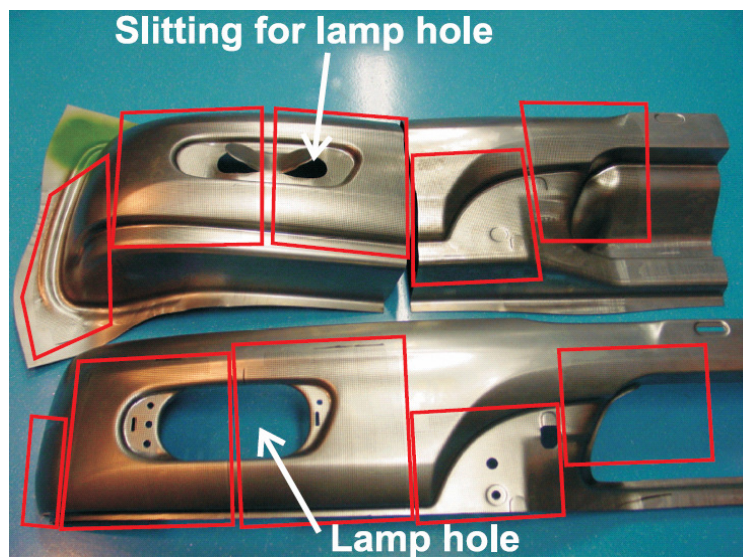


Fig. 12 The etched areas of the finished and semi-finished bumper. Source [7]

As discussed in chapter two a regular grid of dots must be etched onto the unprocessed steel blank. The etching process has been carried out by Kommer [7], who also

performed measurements on the bumper but encountered some difficulties. The dot pattern that has been etched on both bumpers does not cover the complete surface of the bumper and therefore results have been obtained for a few regions. Furthermore, because of symmetry, only half of the bumper is considered. Fig. 12, shows the etched parts on the semi-finished (top) and finished bumper (bottom). For the validation of the LS-Dyna models certain regions were identified, which will be compared with the ARGUS results. These regions are depicted in Fig. 13. The three regions are discussed in the first three sections. The final two sections contain the results of larger measurement areas and the validation of the LS-Dyna results.

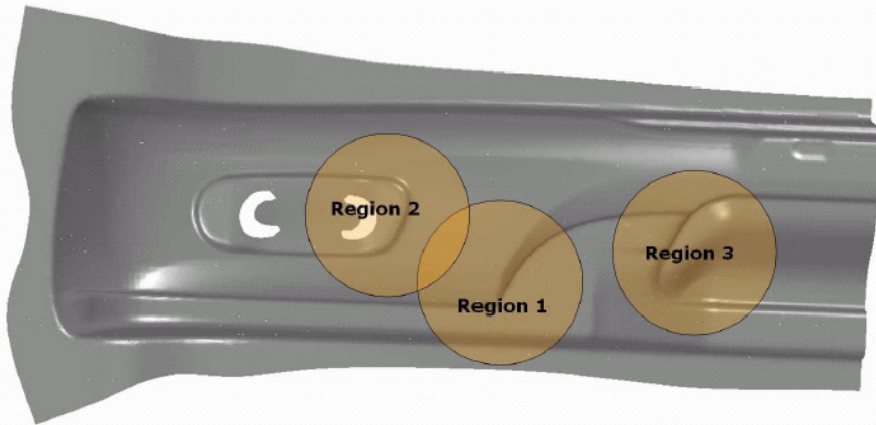


Fig. 13 Three regions for the comparison of the LS-Dyna results. Source [2]

All strains presented in the following are natural, or true logarithmic, strains. The major and minor strains are shown on the object's surface. The major strain is the maximum in-plane principal true strain and the minor strain is the minimum in-plane principal true strain.

The obtained thickness reduction and a Forming Limit Diagram (FLD) are also shown as results. In an FLD the major and minor strain combination, of all nodes of the 3D-grid are represented graphically in a two-dimensional plot. In this plot the combination of major and minor strain for each ellipse is visualized by a dot, where the x-axis represents the minor strain and the y-axis represents the major strain. By introducing a Forming Limit

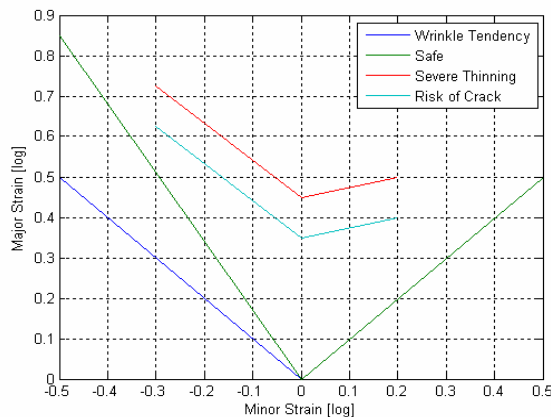


Fig. 14 Forming Limit Curve of the used bumper material.



Curve (FLC) in the same plot, it is possible to see if there are regions with a tendency for forming problems such as wrinkles, severe thinning and cracks. In Fig. 14 the FLC of the used material is shown. Below the blue ‘wrinkle tendency’ line wrinkling of the material may take place. In the area between the blue and the green ‘safe’ line there is a tendency to wrinkle. The area from the green line up to the cyan ‘risk of crack’ line can be regarded as safe. There is a risk of cracking if the strain state lies between the cyan and the red line and above the red line the material is likely to crack.

## 5.1 Results region 1

The two images shown in Fig. 15 represent the major and minor principal natural strain. The scale bar is automatically adjusted in a way that it contains the maximum and minimum value of the strain present in the object. This way of adjusting the scale bar is

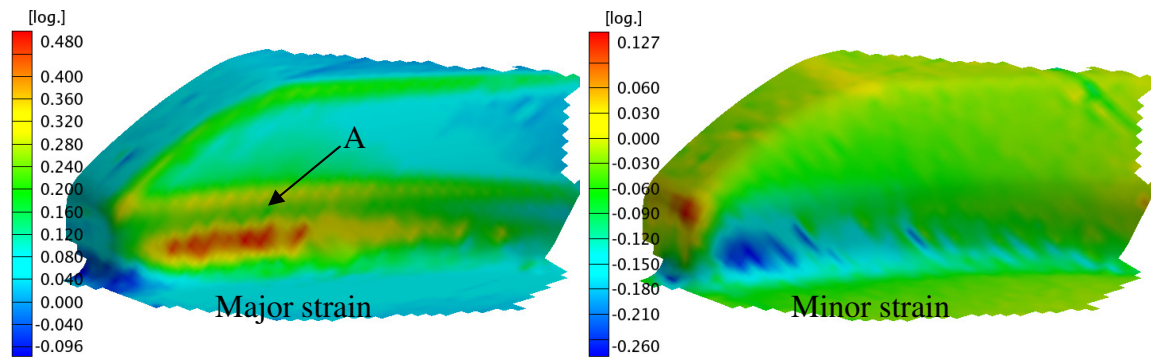


Fig. 15 Major (left) and minor (right) strain for region 1 at surface level.

also used for the other regions. A striking feature is the fact that at point A in the left figure the major strain is lower than the value above and below point A. An explanation for this fluctuation could be that the strain as depicted in Fig. 15 is at surface of the bumper. ARGUS can also calculate the strain in the mid plane of the sheet. The mid plane result is shown in Fig. 16. For good comparison the same scale bar is used. The short black lines represent the major strain direction.

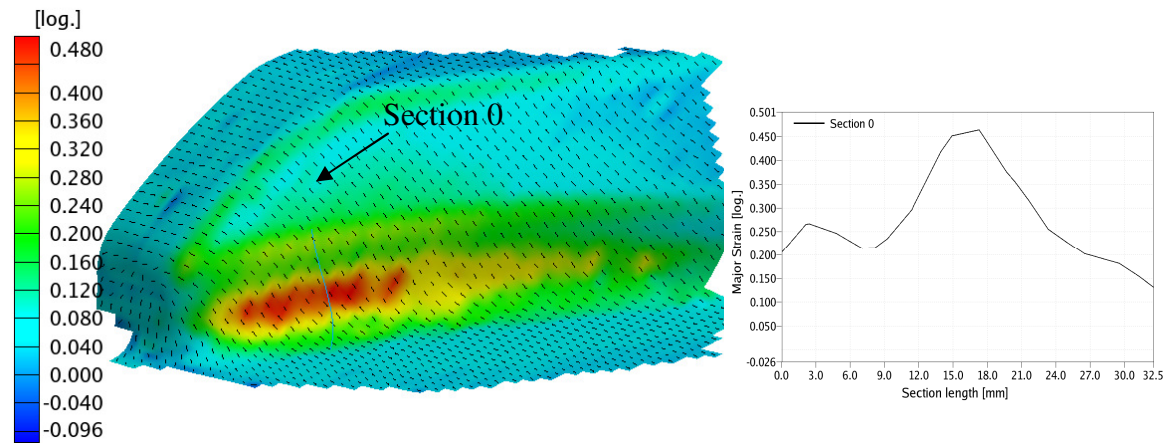


Fig. 16 Major strain and direction in mid plane (left), Major strain multi-section, section 0 (right).

In this mid plane result the major strain in the concave area is higher than the surface strain, whereas in the convex region it is lower. This can be explained by Fig. 17. Pure

bending in the sheet metal results in a positive (tensile) strain at the outside and a negative strain (pressure) at the inside of the curvature. From now on these strains, as depicted in Fig. 17, will be called tangent bending strains. The bending also introduces axial bending strains which have a direction normal to the plane of Fig. 17. The axial bending strains have a negative value at the outside and a positive value at the inside. In the neutral plane, which equals the mid plane for pure bending, the strain as a result of the bending is zero. The major strain at the edge above point A at the surface consists of the mid plane major strain plus the bending major strain. This summation of strain leads to a higher strain value at the surface. It is possible that the principal strain directions change as a result of the bending strains. This will be shown in section 5.4. Even in the mid plane there is still a little fluctuation of the major strain around point A, which clearly can be seen in the multi-section of Fig. 16. This fluctuation is noticeable in the thickness reduction of Fig. 18 as well. It suggests that the sheet was stretched over the die in this region.

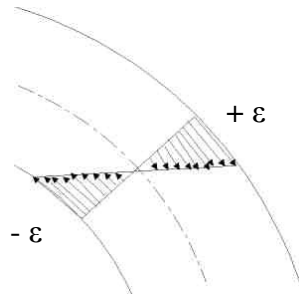


Fig. 17 Strain distribution in case of pure bending.

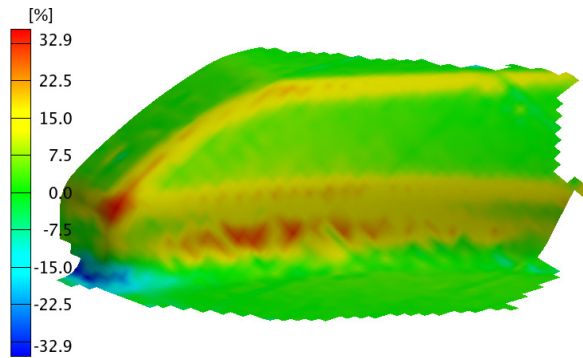


Fig. 18 Thickness reduction of region 1.

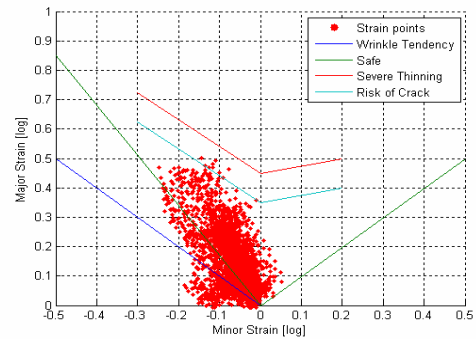


Fig. 19 Forming Limit Diagram of region 1.

The FLD of Fig. 19 shows that some wrinkles are predicted and that at some points there is a risk of cracking. Inspections of the bumper part does not confirm the predicted wrinkles and also no cracks are visible.

## 5.2 Results region 2

In Fig. 20 the major and minor strain distribution of region 2 are shown. Notice the irregularity at point A. This is due to poor interpolation. Point B is an example of a

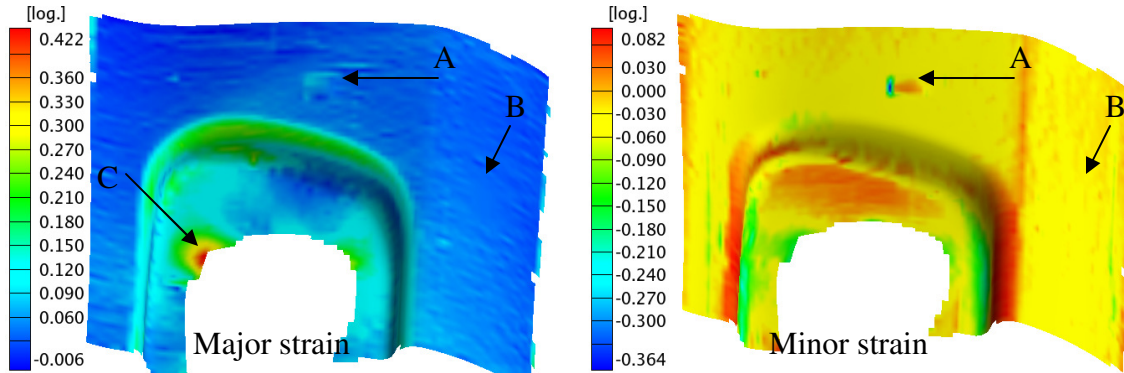


Fig. 20 Major (left) and minor (right) strain for region 2 at surface level.

successful interpolation. In Fig. 21 the major strain distribution is shown without any interpolation and with the same indicated points A and B. At point C in Fig. 20, 21 a highly concentrated strain area is visible. This strain would be even higher if the slitting operation in production step one would be omitted [2].

In Fig. 22 the thickness reduction of region 2 can be seen. Thinning mostly occurs on the bend edges and at point C, where the major strain is the highest. Observing the grid of ellipses at point C, a high strain area is clearly visible. A verification has been done by measuring the dimensions of an ellipse and comparing them with the original dot diameter. This resulted in a major strain at point C of  $\ln(2.5/1.5) = 0.51$ , which is significantly higher than the ARGUS result. Also verification for the thickness reduction at point C has been done. This resulted in a reduction of 27 percent, which is 2.7 percent higher than ARGUS predicts. Finally in Fig. 23 on the next page, the FLD of region 2 shows that there is a risk of wrinkles, which are not visible on the real bumper.

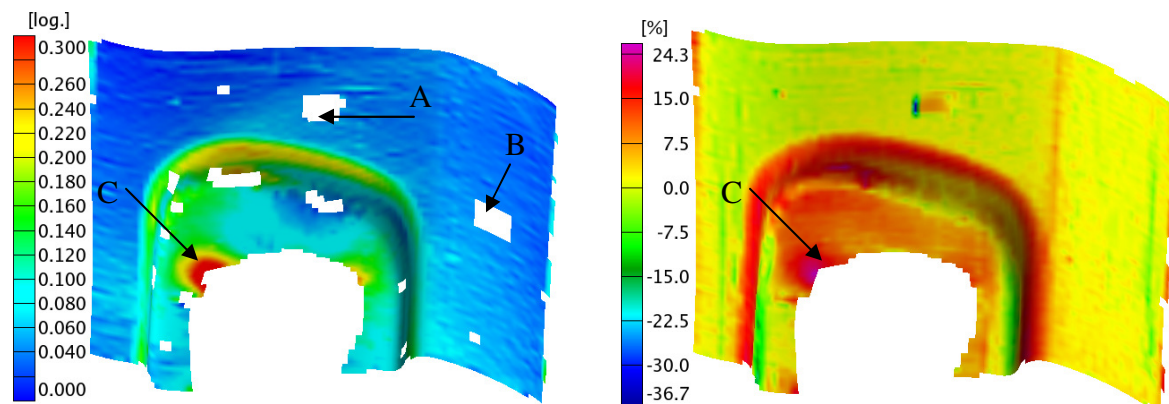


Fig. 21 Major strain of region 2, without interpolation.

Fig. 22 Thickness reduction of region 2.

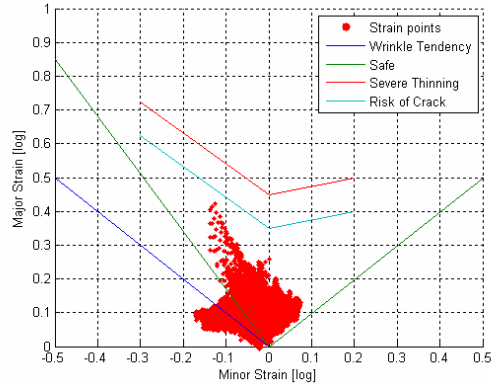


Fig. 23 Forming limit diagram of region 2.

### 5.3 Results region 3

In Fig. 24, the major and minor strain of region 3 are shown. The big gap is due to the fact that the ellipses in that particular area were of low quality. The gap has not been interpolated because it is too big to interpolate it in a meaningful way. In ARGUS it is possible to use filters to smoothen the strain results. To give an example why such filtering is generally undesirable, the major strain result of Fig. 24 has been filtered and plotted in Fig. 25. Just like the previous major and minor strain results the scale bar is automatically adjusted in a way that it contains the maximum and minimum value of the

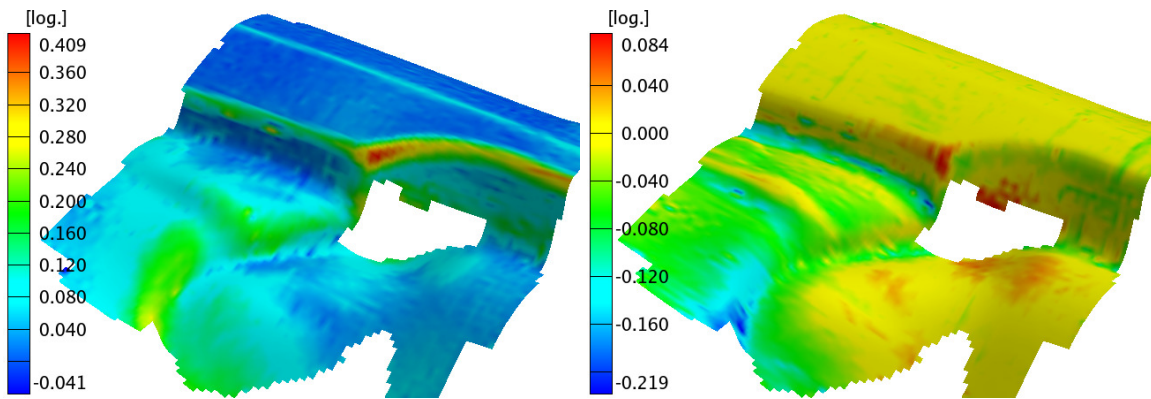


Fig. 24 Major (left) and minor (right) strain for region 2 at surface level.

strain present in the object. The filter has lowered the maximum and raised the minimum value of the strains, and also has an effect on the intermediate strain values. For the maximum strain area the filtered value is 18 percent lower. Therefore, one must be careful using these filters because they manipulate the results. Fig. 26 shows the thickness reduction of region 3.

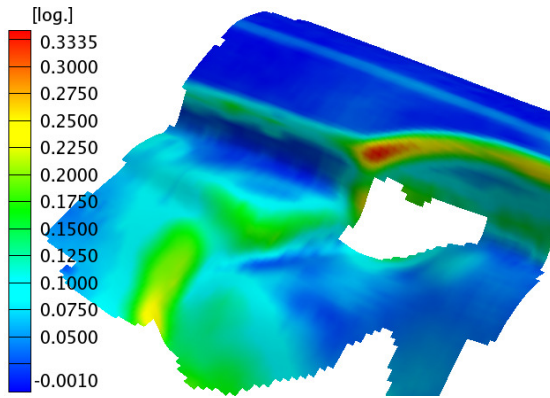


Fig. 25 Filtered result of the major strain of region 3.

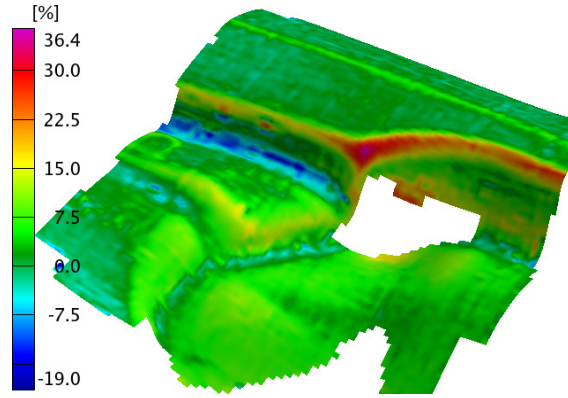


Fig. 26 Thickness reduction of region 3.

## 5.4 Lamphole

Apart from regions 1-3, also the entire lamphole and surroundings has been measured. This measurement has been done for the semi-finished and finished bumper and results are compared in this section. In Fig. 27 the major and minor strain of the semi-finished part can be seen. The gap across the center of the lamphole is due to the fact that the region was etched in two parts, with a 2 cm gap in between. The figure shows very high major strains at points A and B. As mentioned in section 5.2, these strains would be even higher if the slitting operation in production step one were omitted. The somewhat scattered results at point C are due to interpolation of that area. In point D of the minor strain figure a large fluctuation can be seen between the two edges. Fig. 28a shows a close up of this fluctuation in the minor strain and also shows the major strain direction. This major strain direction changes approximately 90 degrees at edge A. This holds for the minor strain direction as well, because it is perpendicular to the major strain direction. This phenomenon is related to the bending strains as described in section 5.1. Unlike the situation encountered there, the bending strains here dominate the strain state at the surface. As a result, the major and minor strain directions are swapped. The major strain direction in the mid plane, where no bending strains are present, is depicted in Fig. 28b. Here the major strain direction is parallel to the edges A and B and does not change between them. At the surface, Fig. 28a, the tangent bending strains introduce a tensile strain at edge A. The tangent bending strains are such that the combination of mid plane strain plus tangent bending strain changes the major strain direction from axial (mid plane) to tangent (surface).

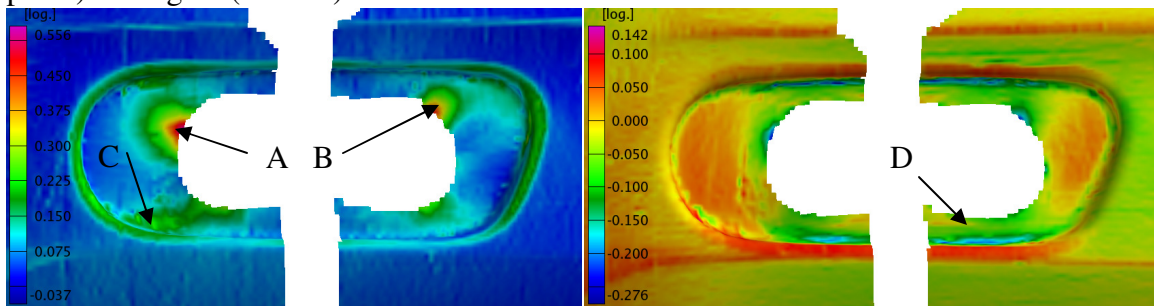


Fig. 27 Major (left) and minor (right) strain for semi-finished lamphole at surface level.

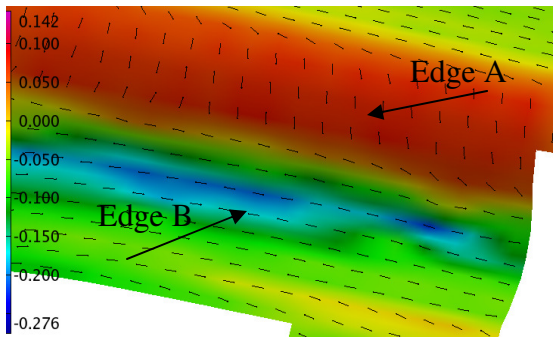


Fig. 28a Minor strain and major strain direction at the surface. Close up of point D.

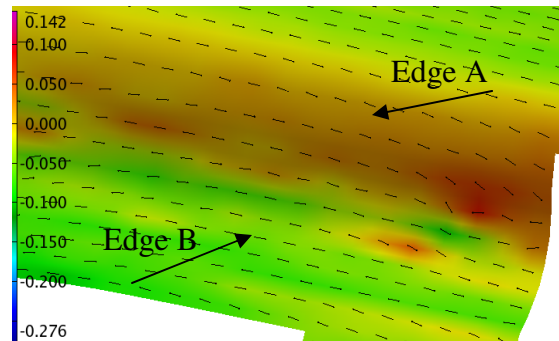


Fig. 28b Minor strain and major strain direction at mid plane. Close up of point D.

The minor strain value at edge A at the surface is higher than at the mid surface because of the switch in principal strain directions. The major strain at the mid plane plus the negative axial bending strain at the surface has become the minor strain at edge A at the surface. For edge B the major and minor strain directions remain the same because the axial bending strain at this edge is positive (tensile) and thus will increase the major strain. Furthermore the negative tangent bending strain at edge B decreases the minor strain, which is also visible by the blue color.

In Fig. 29, the same images are shown for the finished lamphole. The gaps at both sides of the lamphole are holes for the fixation of the lamps etc. The same scale bars are used as with the semi-finished lamphole of Fig. 27, so a good comparison between both production steps can be made. The high major strains at points A and B of Fig. 27 are not present on the finished lamphole because they have been cut away by the slitting operation of the second production step. Otherwise the major strain distribution of the finished part corresponds well with that of the semi-finished lamphole. This also holds for the minor strain. This indicates that the final forming steps introduce relatively little additional deformation and the overall shape of the bumper is largely formed in the first step. The blue areas near point D in the minor strain distribution shown in Fig. 27 are not visible in the finished part because of that particular area no results have been obtained.

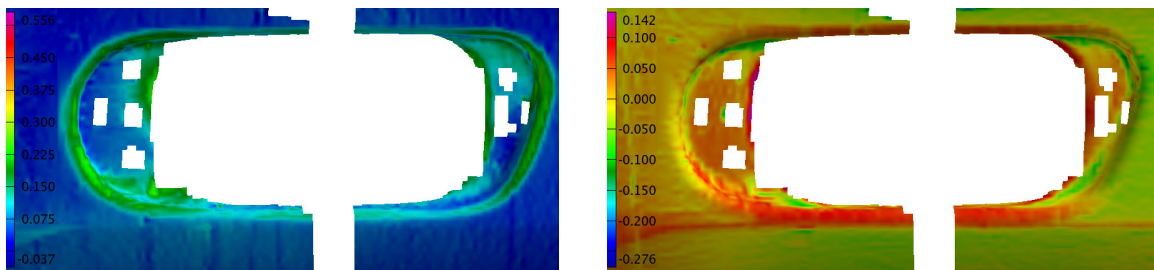


Fig. 29 Major (left) and minor (right) strain for finished lamphole at surface level.

The FLDs of the finished and semi-finished parts near the lamphole can be seen in Fig. 30. The higher strains at point A and B of the semi-finished part are also noticeable in the corresponding FLD. These points, as well as those in the wrinkling regime, are largely removed by the trimming. In the semi-finished part wrinkles are visible near the cutting edges. For the finished part no wrinkles are visible. The last figure of this section, Fig. 31, shows the thickness reduction of the finished part. This diagram shows a limited

amount of thinning, except in the bent region around the lamphole and at the edge of the lamphole, where a significant thinning (approx 25%) has occurred. This corresponds well with the fact that these regions are biaxially stretched (Fig. 29).

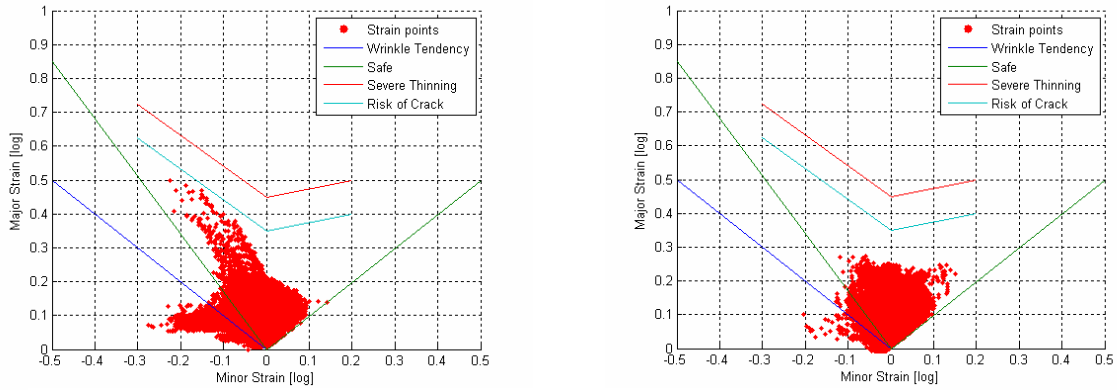


Fig. 30 FLDs for semi-finished lamphole (left) and finished lamphole (right).

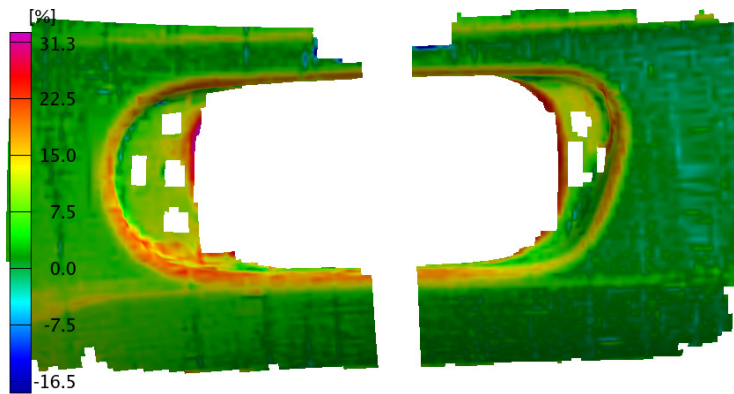


Fig. 31 Thickness reduction of the finished lamphole.

## 5.5 Complete etched region

The final measurement that has been done is of the complete finished bumper, or to be more precise, of that part of the bumper (approx 40%) which was etched before forming. The results are acceptable, but they could have been better if more diffuse light and a

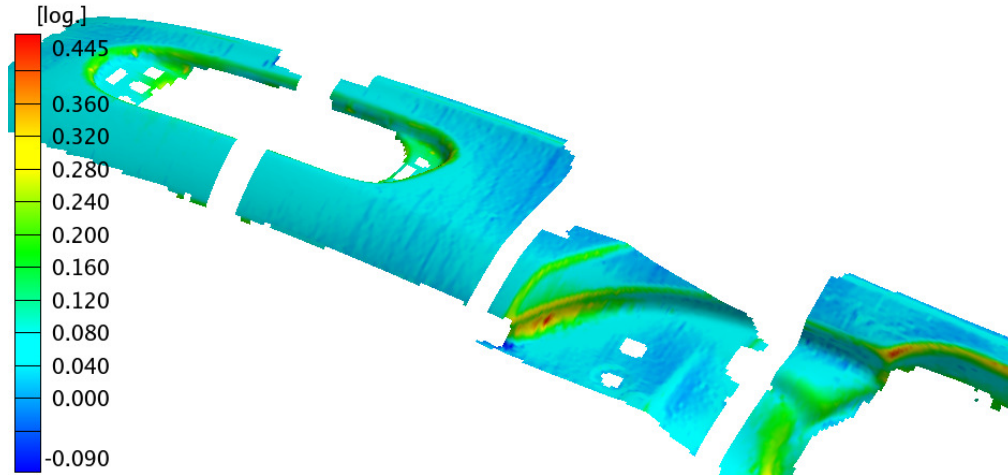


Fig. 32 Major strain at the surface of the complet bumper.

better digital camera with a higher resolution were available. Due to the lack of diffuse light the curved areas were underexposed, resulting in a lower grid quality than in the previous measurements. In Fig. 32 the result of the major strain is shown. Because not the complete bumper has got the etched dot pattern, certain areas have no grid and thus have no strain information. In Fig. 33 below the minor strain of the total bumper can

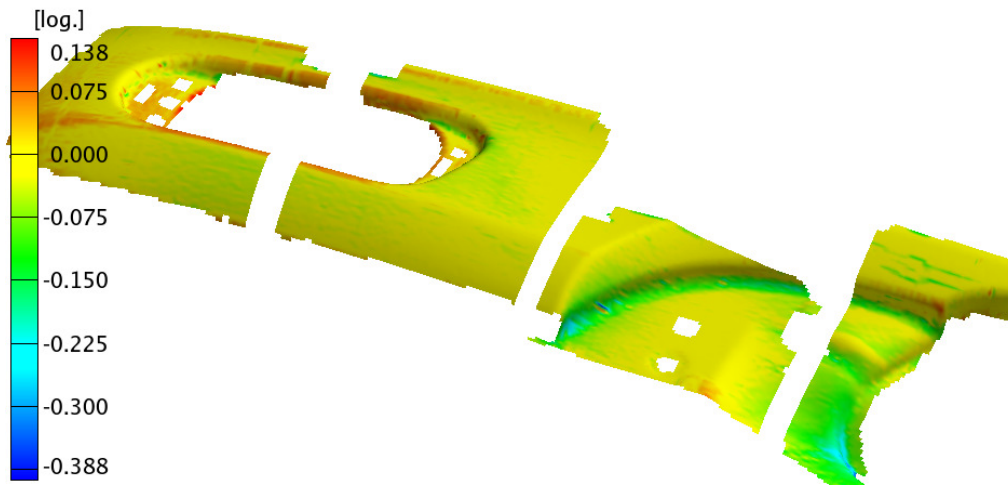


Fig. 33 Minor strain at surface level of the total bumper.

be seen. The correspondence between the total bumper results and the smaller sized results is reasonable. Differences must be attributed to the insufficient lighting of the entire bumper resulting in underexposed areas. In the highly strained areas this may lead to errors of approximately 25 percent. It is believed to be feasible to do a measurement of larger objects if enough diffuse light is guaranteed and a better digital camera is used.



Fig. 34 shows the FLD of the complete bumper. It suggests that wrinkles are definitely present and that there is a risk of cracking for a few points. However, no wrinkles or cracks are visible on the real bumper.

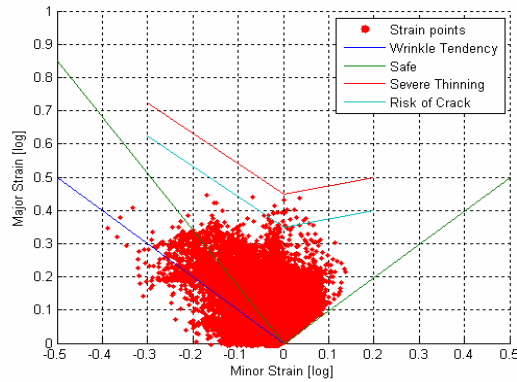


Fig. 34 FLD of complete finished bumper.

## 5.6 Validation of the LS-Dyna results

Now the strain results of the different regions are available it is possible to compare the forming simulation results (using LS-Dyna) with the ARGUS measurements. The used regions for this validation are depicted in Fig. 13 on page 15 and belong to the semi-finished bumper. The ARGUS and LS-Dyna results are at the mid plane. In some small areas of the ARGUS results interpolations have been carried out. It will be mentioned if these interpolations give an unrealistic or peculiar effect. More information about the LS-Dyna models and forming process can be found in [2].

### Region 1

In Fig. 35 below, the major and minor strains of region 1 are compared. The fluctuation at point A, which was discussed in section 5.1, is not visible in the LS-Dyna results.

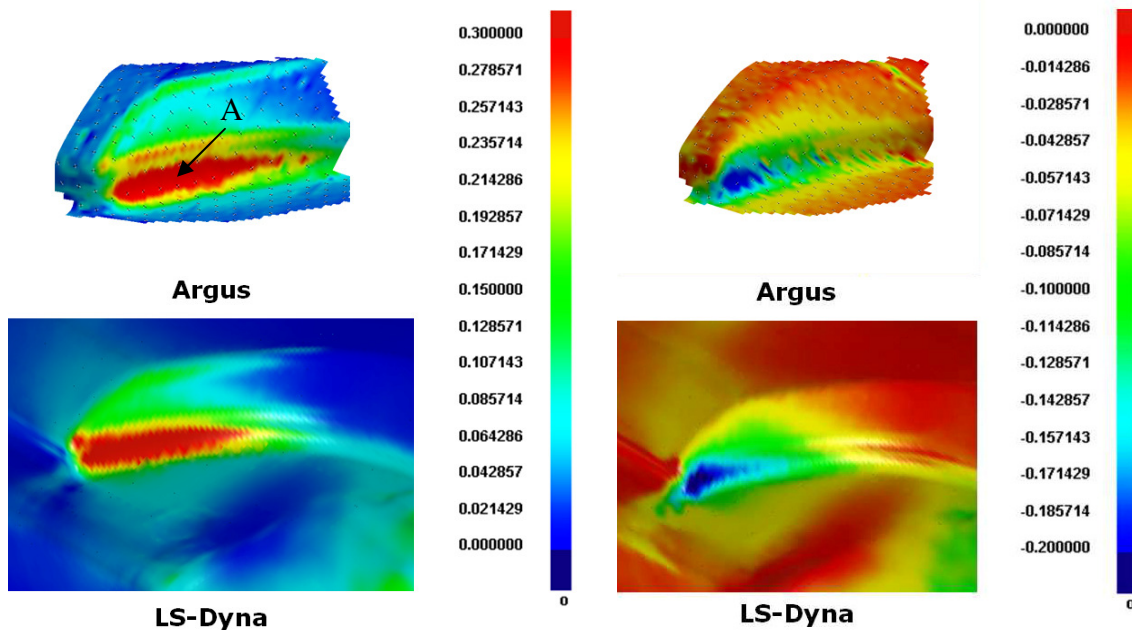


Fig. 35 Comparison between LS-Dyna and ARGUS for region 1. Left: major strain; right: minor strain.

In this and other regions, the LS-Dyna results are much smoother than those of ARGUS. In ARGUS it is possible to create such smooth results by using a filter. But, as mentioned in section 5.3, it will lower the maximum strain values in a more or less arbitrary way. The small fluctuations of the ARGUS results are only visible in the low strain regions. The fluctuations have A wavelength which approximately equals the grid spacing and are probably measurement errors with an absolute error of approximately  $0.02 \epsilon_{ln}$ . Apart from the fluctuations in the ARGUS result, the general agreement between measurement and simulation is remarkable.

### Region 2

The results of region 2 are shown in Fig. 36. The arrows indicate areas where interpolation has been used and gave an irregular strain pattern. Besides these points the

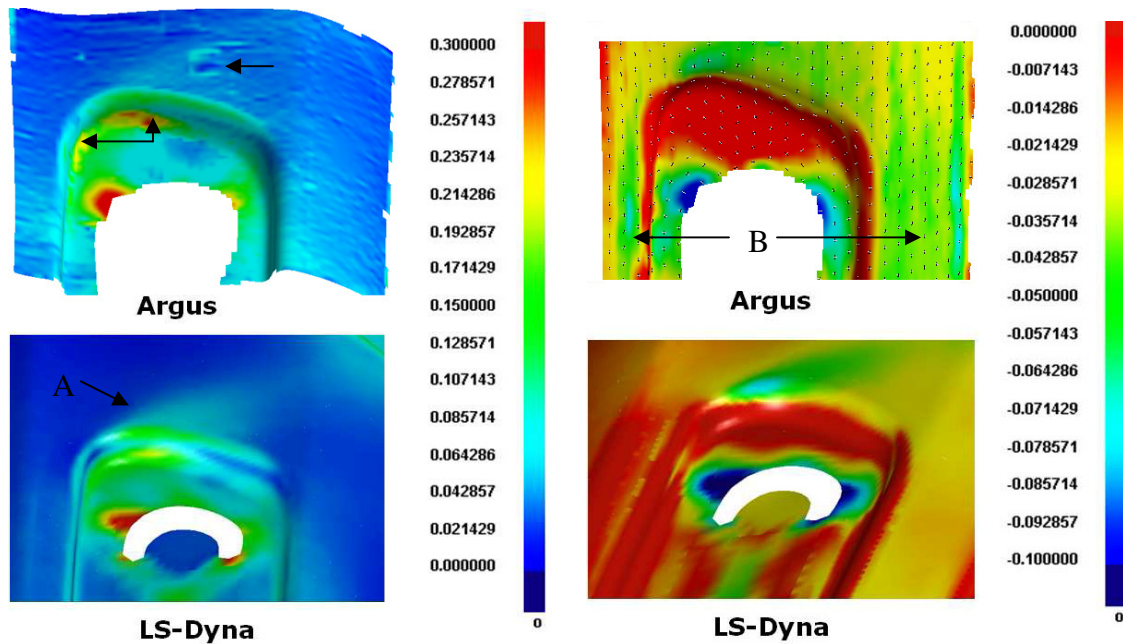


Fig. 36 Comparison between LS-Dyna and ARGUS for region 2. Left: major strain; right: minor strain.

major strain resemblance is good. Even the shade of light blue at point A of the LS-Dyna result is confirmed by the ARGUS image. For the minor strain the correspondence is slightly poorer. Especially above and below the lamphole, indicated by B, where the LS-Dyna result seems to be higher than measured by ARGUS.

### Region 3

The images of the last region can be seen in Fig. 37. The big gap in the ARGUS image of both major and minor strain is due to poor ellipse quality in that area. Interpolating such a gap is unacceptable because it will generate a nonphysical strain field. The few spots near point A are another example of an interpolation error. The remainder of the major and minor strain correspondence between ARGUS and LS-Dyna is again satisfactory.

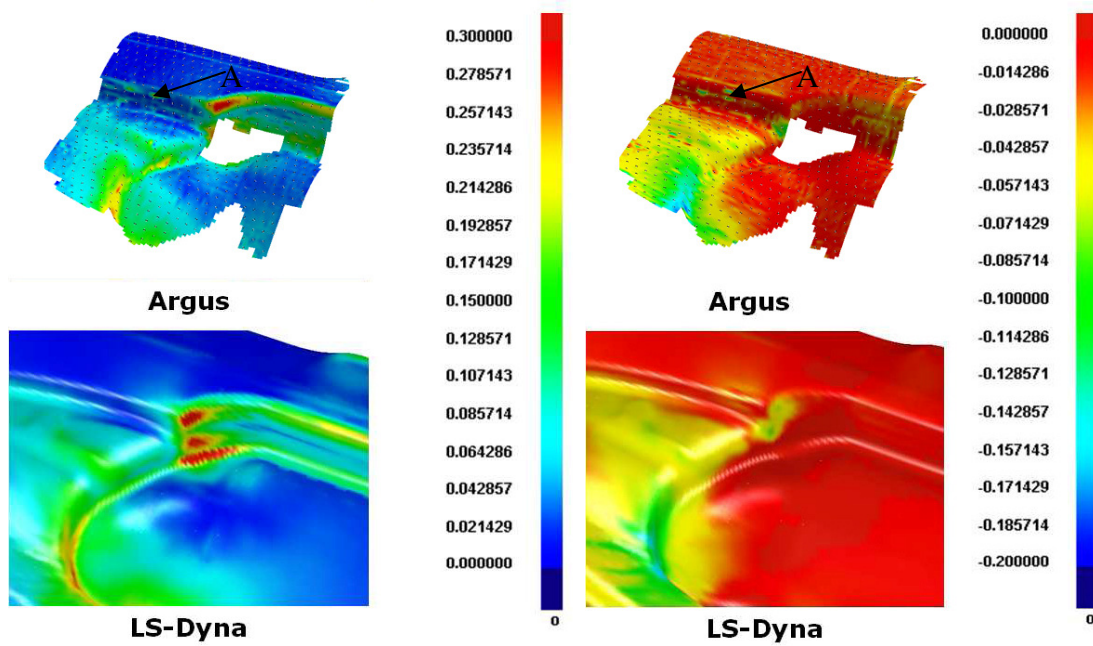


Fig. 37 Comparison between LS-Dyna and ARGUS for region 3. Left: major strain; right: minor strain.

# Chapter 6

## Conclusion and recommendations

The main requirements for an accurate strain measurement using ARGUS is a set of proper digital pictures. This can be established by correct illumination, marker positioning and proper camera use:

- The illumination of a measurement object must be diffuse to reduce reflections and must result in a homogeneous light distribution, covering the complete object. Preferably the measurement should be done in a dark room so that no external light can influence the controlled illumination.
- The markers have to be distributed around the area to be measured in such a way that at least five markers are visible from each perspective. These markers may not form a straight line and preferable should not all lie in the same plane. During the measurement, the markers may not be moved with respect to each other and to the etched pattern on the sheet metal
- The following camera settings are important for the ARGUS system and must be entered correctly: pixel size, pixel resolution and focal length of the camera. Extra care must be taken with the latter because it changes if the zoom function is used. Therefore it is advisable not to zoom during a measurement. One should realize that these settings are of great importance because they are used in the photogrammetric computations.
- Measuring large objects is feasible if a proper illumination setup is used. The currently available illumination is sufficient for small and medium sized objects and individual measurement regions of the bumper. Because of a lack of diffuse light this setup is insufficient for large measurement objects such as the complete bumper.

With large objects it may be necessary to take photographs from a greater distance, resulting in a change of the number of pixels that an ellipse contains. The diameter of an ellipse must be between approximately five and ten pixels. The camera resolution should then be sufficient to be able to have the ellipse diameter between its limits or larger dots should be used.

The results in this study demonstrate two more important aspects of the measurement:

- One must be careful using filters that smoothen the results because they lower the maximum and raise the minimum value of the strains, possibly creating a nonphysical strain field. ARGUS is equipped with three different types of filters with accompanying settings. These filters and settings have not been investigated enough in this study but may be of interest in another study.
- Also care must be taken in using the interpolation tool to fill up gaps in the grid. Only make use of it if the gap is small and the strain has no rapid changes in that particular region.

The results of the individual regions are quite satisfactory, but they could have been better for the complete bumper if the illumination were sufficient. Also the LS-Dyna results correspond well with the ARGUS results.

In this study measurements have been done of the complete etched region of the bumper and of the individual regions. In the latter the measurement areas are still relatively large and the used grid pattern was always the same. Some external measurements have been performed for a different project where a fine grid was used and the measurement area was small. These measurements gave some problems which could not directly be solved by the knowledge obtained in this study. Therefore it may be useful to investigate some small scale measurements with different grid sizes.

# Bibliography

1. A. Aydemir, *Forming to crash – Process simulation of DAF bumper 10680*, Netherlands institute of metal research, April 2006, Nieuwegein
2. T. van Hoek, *The history influence of forming on the predicted crash performance of a truck bumper*, Technical University Eindhoven, August 2006, Eindhoven [MT06.36]
3. GOM optical measuring techniques, *ARGUS – Sheet metal forming measuring system – Introduction (v 4.7)*, GOM GmbH, 2001, Braunschweig
4. GOM optical measuring techniques, *ARGUS – abridged user manual (v 5.4)*, GOM GmbH, 2005, Braunschweig
5. Website of University of Vienna ‘Introduction to Photogrammetry’ url: <http://www.univie.ac.at/Luftbildarchiv/wgv/intro.htm>
6. Wikipedia, Free Encyclopedia *Photogrammetry* url: <http://en.wikipedia.org/wiki/Photogrammetry>
7. N. Kommer, *Optical strain measurement on a DAF truck bumper*, Technical University Eindhoven, December 2006, Eindhoven [MT06.53]